

Electron-hole recombination properties of $\text{In}_{0.5}\text{Ga}_{0.5}\text{As}/\text{GaAs}$ quantum dot solar cells and the influence on the open circuit voltage

Greg Jolley,^{a)} Hao Feng Lu, Lan Fu, Hark Hoe Tan, and Chennupati Jagadish
*Department of Electronic Materials Engineering, Research School of Physics and Engineering,
 The Australian National University, Canberra, ACT 0200, Australia*

(Received 18 July 2010; accepted 2 September 2010; published online 23 September 2010)

We report on a detailed analysis of the temperature dependent electrical properties of $\text{In}_{0.5}\text{Ga}_{0.5}\text{As}/\text{GaAs}$ quantum dot solar cells. The effects leading to a reduction in the open circuit voltage are found to be the thermal injection of carriers from the n and p-type layers into the depletion region where they recombine with carriers occupying quantum dot states due to a thermal distribution. The departure of the device studied here from an ideal intermediate band solar cell is discussed. © 2010 American Institute of Physics. [doi:10.1063/1.3492836]

The intermediate band (IB) solar cell was proposed as a way of breaking the efficiency limits of a single junction device.¹ Theoretical studies have suggested a maximum efficiency of 63.1% under full concentration¹⁻⁴ compared with 40.7% for a single junction device. Quantum dots (QDs) have been favored for the formation of an IB due to the possible thermal decoupling of the discrete density of states from the bulk states.⁵ A number of QD solar cells have been reported in an attempt to demonstrate an IB device. So far all reported experimental efficiencies of QD solar cells have been less than that of the best GaAs single junction devices.⁶⁻¹¹ Although including QDs within the device absorption region has been reported to increase the short-circuit current density (J_{sc}), the open circuit voltage (V_{oc}) has always been degraded. The relationship between the QD band structure and V_{oc} has been debated in the literature and is not well known. In addition there is uncertainty regarding how far realistic QDs that can be grown with currently available technology are from the conditions, or assumptions outlined in reference¹ in the analysis of the efficiency potential of IB solar cells. The general consensus is that the QD states need a quasi-Fermi level that is separated from the bulk Fermi levels to maintain a V_{oc} that is determined by the band gap of the host material rather than the QD band gap. This requires the QD energy states to be thermally decoupled from the bulk states. The necessity of electronic coupling between QD layers for the formation of an IB with a separate Fermi level has recently been questioned.⁹

For this work, we report on a detailed analysis of the temperature dependent recombination properties of $\text{InGaAs}/\text{GaAs}$ QD solar cells. From this analysis the effects leading to a reduced V_{oc} are determined which is important for the development of high efficiency QD solar cells. A QD and reference solar cell device were grown by low-pressure metal-organic chemical vapor deposition on n-doped (001) oriented GaAs substrates. Growths began with the deposition of a 200 nm n+GaAs buffer layer and 200 nm n-doped GaAs base layer. The reference cell consists of an absorbing region of 500 nm of unintentionally doped GaAs whereas the QD device consists of 10 QD layers each separated by 50 nm of GaAs. A 200 nm GaAs p-doped emitter, 30 nm $\text{Al}_{0.45}\text{Ga}_{0.55}\text{As}$ window, and 100 nm p+GaAs top contact cap

the absorption region. The performance characteristics of the QD device will only be a true representation of the QD physics if the device is free from the defects which can potentially form from the lattice mismatched Stranski-Krastanov growth mode. The QD growth parameters have previously been optimized¹² and the solar cell displays a strong room temperature photoluminescence response indicating that the QDs have high optical quality (see insert of Fig. 1). After growth wafers were processed into $3 \times 3 \text{ mm}^2$ mesa devices using contact UV lithography and wet chemical etching. Top Ohmic contacts were formed by the thermal evaporation of Au and a lift-off process. Bottom Ohmic contacts were formed by evaporating Ge/Au onto the back of the substrate. After metallization the top 100 nm GaAs contact layer that is exposed to light was removed by selective etching. Devices were characterized without the addition of antireflection coatings.

A temperature dependent study of the spectral response and light I-V characteristics allows an investigation into the effects of recombination on the solar cell electrical properties since the amount of recombination widely varies with temperature.¹³ Spectral response measurements were performed using a tungsten lamp, monochromator, and mechanical chopper with the devices biased with a current pre-amplifier connected to a lock-in amplifier. Measurements

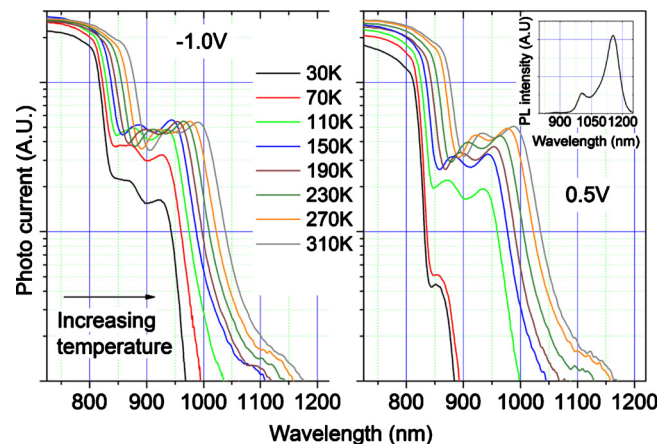


FIG. 1. (Color online) The spectral response of the QD solar cell for various temperatures and an applied bias of -1.0 and 0.5 V. The insert plot is the room temperature photoluminescence spectrum of the QD device.

^{a)}Electronic mail: gregory.jolley@anu.edu.au.

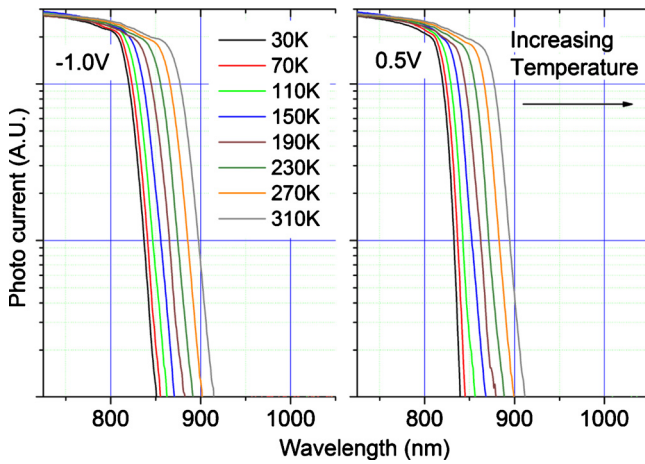


FIG. 2. (Color online) The spectral response of the reference solar cell for various temperatures and an applied bias of -1.0 and 0.5 V.

were done with an applied bias of -1.0 and 0.5 V and the results are shown for the QD and reference devices in Figs. 1 and 2, respectively. The room temperature photoluminescence spectrum of the QD device shown in the insert of Fig. 1 which displays a QD ground state recombination peak at 1160 nm and a wetting layer recombination peak at 1000 nm can be correlated with the device photocurrent spectrum. A QD ground state photocurrent response at 1160 nm is clearly visible at the higher temperatures but is small due to the intrinsically weak QD absorption cross section. The two peaks in the QD device spectral response which are located at 990 and 935 nm at room temperature are due to wetting layer transitions. For photogenerated carriers to result in an external current they must cross the intrinsic region and join the majority carriers in the contact layers. For a QD device that does not form a mini band, carriers in the bound states can escape a QD layer by either photon or phonon excitation to barrier states or by direct tunneling to neighboring layers. Direct tunneling through thick barrier regions is a relatively slow process and therefore either thermal or optical excitation of carriers out of the QDs are the important processes for the device studied here. For the small optical intensities used in the spectral response measurements (and for unconcentrated sunlight) the optical excitation rate of carriers out of the bound states would also be a relatively slow process leaving thermal excitation as the dominant process. Carriers in the depletion region undergo two main competing processes, (1) thermal excitation out of the bound QD states and subsequent drift in the depletion region electric field and (2) capture from barrier states to QD states with possible radiative recombination. The carrier escape time constants are very sensitive to temperature and it is expected that they become short compared with the radiative recombination lifetime of the carriers in bound states beyond some temperature. Also, the capture probability is dependent on the electric field. Therefore the amount of recombination of the photocurrent should be sensitive to both the temperature and external bias. The QD device clearly exhibits this behavior. At low temperatures, particularly for wavelengths that create electron-hole pairs directly bound to either QDs or the WL, the amount of recombination becomes a considerable fraction. Near room temperature the spectral response has a weak dependence on the temperature and bias suggesting that little recombination is taking place. The main device parameters

TABLE I. The main device parameters.

Device	Jsc (mA/cm ²)	Voc (V)	η (%)	FF (%)
QD	18.2	0.791	11.2	77.9
Ref.	18.3	0.995	15.3	83.8

were obtained under standard AM1.5G conditions using a solar simulator, the results are shown in Table I. The short circuit current density of the QD device is about 0.5% less than the reference cell indicating that a small amount of recombination of carriers is occurring at room temperature. However, Voc of the QD device is about 20% less than that of the reference cell.

Temperature dependent light I-V measurements were also performed to investigate the effects of the recombination on Voc and the total device current which consists of both the photocurrent and the current injected from the n and p-type layers (defined here as forward injection current), the results of which are shown in Fig. 3. Two important effects can be seen, namely, a large amount of voltage dependent recombination of photocurrent results in a poor fill factor and Voc of the QD and reference devices are very similar at lower temperatures. The probability that photocarriers are captured into QD layers and their escape rate from these bound states are both expected to be electric field dependent resulting in a voltage dependent recombination and therefore a poor fill factor, particularly at lower temperature. In spite of the large amount of recombination of the photocurrent, Voc of the QD device is very similar to the reference cell at low temperatures and is determined by the built in potential, V_{bi} , which is equal to the splitting of the Fermi levels of the base and emitter layers $V_{bi}=(E_{Fn}-E_{Fp})$. This indicates that the reduction in the QD device Voc at higher temperatures is the result of the thermal injection of carriers into QD layers and subsequent recombination within the depletion region. A schematic demonstrating the basic effects leading to a reduction in the Voc is shown in Fig. 4.

Assuming a parabolic band structure, carriers in the contact layers have the following kinetic energy distribution $P(E) \propto \sqrt{E} \exp(-E/k_bT)$, where $P(E)$ is the probability that a carrier has the kinetic energy E , k_b is the Boltzmann constant, and T is the solar cell temperature. Carriers from the

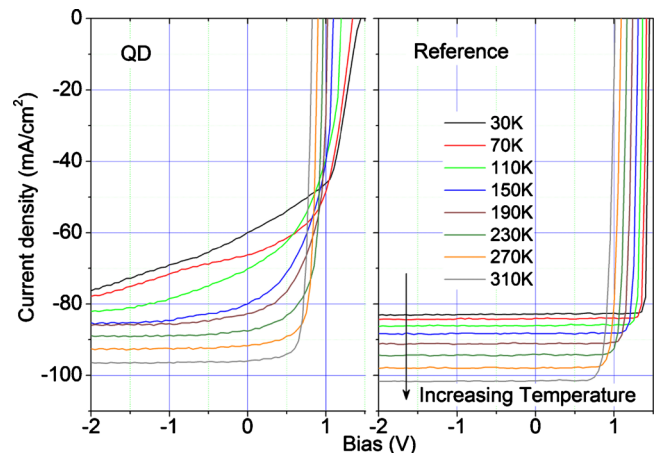


FIG. 3. (Color online) The current-voltage curves of the QD and reference solar cell exposed to light from a tungsten lamp for various temperatures.

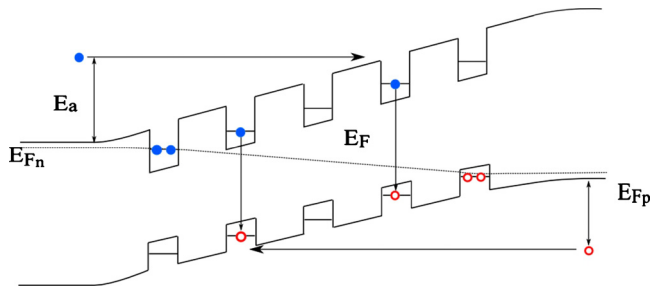


FIG. 4. (Color online) Band diagram demonstrating thermal injection of carriers into QD layers and subsequent recombination, leading to a reduction in the forward current thermal activation energy and hence V_{oc} .

contact layers with sufficient kinetic energy incident upon the depletion region can either cross it and recombine in the opposite contact layer, or recombine somewhere within the depletion region. The forward injection current thermal activation energy (E_a) for carriers crossing the depletion region is $E_a = V_{bi} - V$, where V_{bi} is the built-in voltage which is determined by the Fermi levels in the base and emitter regions ($E_{Fn} - E_{Fp}$) and V is the external potential across the cell contacts. If the forward device current is dominated by recombination within the depletion region the activation energy will be smaller than $V_{bi} - V$ since less thermal energy is required for carriers to only partially cross the depletion region. For the QD device electrons from the base and holes from the emitter region can occupy QD layers under quasi thermal equilibrium conditions, particularly the first couple of QD layers near the contacts. Minority carriers captured by these QD layers will have a greater spatial overlap with majority carriers and a high probability of recombination. Aside from the external bias and temperature, the population of the QD layers will depend on the QD density and band structure which will influence the depletion region recombination current. Therefore V_{oc} is expected to depend on the QD parameters. Calculations of the dark forward current thermal activation energy from measured data confirms that the QD device has a significantly reduced E_a indicating recombination within the QD layers. The activation energies were calculated for device current densities between 10 and 100 mA/cm² with device temperatures ranging between 270 and 310 K. The activation energies of the reference and QD devices were found to be about $1.3 - V$ eV and $1.1 - V$ eV, respectively, where V is the applied bias. The difference corresponds closely with the difference in V_{oc} as determined by measurements with the solar simulator. At low temperature the device current is dominated by the built in potential

which is the same for the reference and QD devices and therefore V_{oc} is very similar for $T = 30$ K.

Our analysis and conclusions are consistent with the main device parameter results of Ref. 11 where a significant reduction in V_{oc} is only observed if QD layers are inserted into the depletion region, Where QDs were grown within either the emitter or base layer a large V_{oc} was maintained even though a large reduction in the J_{sc} was observed because of an enhanced minority carrier recombination within the QD bound states, particularly for the case where the QDs were grown within the emitter layer.

In conclusion, we have demonstrated that the reduction in V_{oc} for QD solar cell studied here and other similar structures is due to the injection of carriers from the contact layers into the active region and subsequent recombination with carriers in quasithermal equilibrium with barrier states. Improvements in QD growth to produce fewer bound states with larger energy spacings is needed to increase the thermal decoupling between the QD and barrier states to increase V_{oc} .

Thanks are due to the Australian Research Council for the financial support of this research and the Australian National Fabrication Facility for access to the facilities used in this work. The authors thank Dr. Rao Tatavarti for interesting and fruitful discussions.

¹A. Luque and A. Marti, *Phys. Rev. Lett.* **78**, 5014 (1997).

²A. Marti, L. Cuadra, and A. Luque, *IEEE Trans. Electron Devices* **48**, 2394 (2001).

³R. Strandberg and T. W. Reenaas, *J. Appl. Phys.* **105**, 124512 (2009).

⁴A. Marti, L. Cuadra, and A. Luque, *IEEE Trans. Electron Devices* **49**, 1632 (2002).

⁵V. Popescu, G. Bester, M. C. Hanna, A. G. Norman, and A. Zunger, *Phys. Rev. B* **78**, 205321 (2008).

⁶D. Alonso-Álvarez, A. G. Taboada, J. M. Ripalda, B. Alen, Y. Gonzalez, L. Gonzalez, J. M. Garcia, F. Briones, A. Marti, A. Luque, A. M. Sanchez, and S. I. Molina, *Appl. Phys. Lett.* **93**, 123114 (2008).

⁷S. M. Hubbard, C. D. Cress, C. G. Bailey, R. P. Raffaele, S. G. Bailey, and D. M. Wilt, *Appl. Phys. Lett.* **92**, 123512 (2008).

⁸R. B. Laghumavarapu, M. El-Emawy, N. Nuntawong, A. Moscho, L. F. Lester, and D. L. Huffaker, *Appl. Phys. Lett.* **91**, 243115 (2007).

⁹D. Guimard, R. Morihara, D. Bordel, K. Tanabe, Y. Wakayama, M. Nishioka, and Y. Arakawa, *Appl. Phys. Lett.* **96**, 203507 (2010).

¹⁰D. Zhou, G. Sharma, S. F. Thomassen, T. W. Reenaas, and B. O. Fimland, *Appl. Phys. Lett.* **96**, 061913 (2010).

¹¹D. Zhou, P. E. Vullum, G. Sharma, S. F. Thomassen, R. Holmestad, T. W. Reenaas, and B. O. Fimland, *Appl. Phys. Lett.* **96**, 083108 (2010).

¹²P. Lever, H. H. Tan, and C. Jagadish, *J. Appl. Phys.* **95**, 5710 (2004).

¹³A. Zachariou, J. Barnes, K. W. J. Barnham, J. Nelson, E. S. M. Tsui, J. Epler, and M. Pate, *J. Appl. Phys.* **83**, 877 (1998).